Solar Physics
DOI: 10.1007/•••••-•••-•••-••••-•

Photospheric Signatures Of Solar Flares

Priya Desai[1] · **Richard Bogart**[1] ·
Sebastien Couvidat[1] · **Hugh Hudson**[2] ·
Jesper Schou[1]

Abstract We investigate flare-related changes in a photospheric absorption line (Fe I 617.3 nm) profile in several solar flares of varying X-ray and H-α classes, observed with the Helioseismic and Magnetic Imager (HMI) instrument aboard the Solar Dynamics Observatory (SDO).

We present observations from four X-ray flares: SOL2011-02-15T01:56 (X2.2) flare which shows distinct continuum and line-core brightening; SOL2011-09-07T22.38 (X1.8) which exhibits significant continuum and more pronounced line core brightening; SOL2011-09-24T09:40 (X1.9) where the line-core exceeds the continuum such that the absorption line briefly reverses and goes into emission (a phenomenon that may have been observed before, but not in such high resolution); and, SOL2010-11-04T23:58:00 (M1.6) which shows less pronounced line-core brightening and continuum enhancement. In no case do we see significant polarization in the continuum emission. We note that although the HMI produces high resolution line-of-sight (LOS) observables including continuum intensity, line width, and line depth at a 45 second cadence, the algorithm used to interpret the level 1 HMI filtergrams is based on assumptions that may not be valid during impulsive phenomena like flares. In such cases it is imperative that we use the level 1 filtergrams for analysis; the LOS observables are at best useful only for cursory diagnostics.

Keywords: Solar Dynamics Observatory, continuum, absorption line, photosphere, white-light flares, HMI

1. Introduction and Motivation

A solar flare is an explosive release of energy stored in twisted magnetic fields, usually above or near sunspots. The term white-light flare (WLF) has traditionally been used to designate solar flares observable as transient brightenings in the visible continuum (Carrington, 1859). WLFs are important in flare research

[1] Stanford University, Stanford, CA, USA;
email:priya@solar.stanford.edu
[2] Space Sciences Laboratory, University of California,
Berkeley, CA, USA

because the continuum represents a large fraction of the radiated energy of a flare (e.g., Neidig, 1989), and their properties challenge our current understanding of flare energy transport (e.g. Krucker et al., 2011).

It is currently believed that the visible continuum is enhanced in all flares, but that the weaker ones are not detected as the signal is lost in the normal spatial and temporal fluctuations of the photosphere. Furthermore, even in strong flares, if of small spatial extent (<5 Mm), and of short duration (<250 s), a systematic observation of the white-light component of flares has been historically challenging. It is difficult to capture a flare serendipitously at the right time and location for a spectroscopic observation, and most measurements (including space-based ones) do not have the spatial and temporal resolution to observe the WL continuum near sunspots, which have large image contrast. In fact, prior to 1993 (Neidig, Wiborg, and Gilliam, 1993), only ∼86 WLFs had been reported, and white-light emissions were only detected in flares above GOES magnitude X2. Surveys of white-light flares observed by Yohkoh (Matthews *et al.*, 2003) and by Hinode (Wang, 2009) found the detectability threshold to be around class M1 flare. Hudson, Wolfson, and Metcalf (2006) used white-light observations from the Transition Region and Coronal Explorer (TRACE) with a spatial resolution of 1″ and detected white-light emission for events as weak as GOES C2.0. Jess *et al.*, (2008) detected intense white-light emission in the blue continuum for a C1.6 flare using the diffraction-limited observations of the Swedish 1-meter Solar Telescope.

Motivated by the renewed interest in white-light flares, which we define as flares exhibiting enhanced emission in parts of the spectrum originating at or near the height of the visible continuum photosphere, we set out to determine if we could detect photospheric flare signatures using the Helioseismic and Magnetic Imager (HMI) instrument (Schou *et al.*, 2012) on the Solar Dynamics Observatory (SDO), launched on February 11, 2010. The HMI instrument provides images in a photospheric line, Fe I 617.3 nm, at sufficient spatial and temporal resolution to resolve flare signatures and provide continuous images during the flare. Measurements of the line strength and nearby continuum brightness along with Doppler and polarization information, and covering the whole solar disc, are available at a spatial scale of 0.5" once every 45 sec. Full-disc filtergrams are available every 3.75 sec, in one of two polarization states, and one of six wavelengths across the line, offering the potential of high time resolution of the photospheric signatures of solar flares, provided that they can be detected and adequately measured. Thus, we have an opportunity to study the profiles of a large sample of flares of varying magnitudes using the same instrument, unlike previous ground based observations, which typically were with slit spectrographs providing limited coverage (e.g. Neidig, 1989) and variable observing conditions.

The HMI capability provides a first opportunity to study the behavior of the line profile systematically. Specifically we would like to understand emission in the line itself, along with the nearby continuum, as a more complete guide to the photospheric participation in the flare.

Table 1. Characteristics of the flares chosen for this study.

Date	Peak (UT)	AR	Location	Class	Comments
2010.11.04	23:58	11121	S20 E76	M1.6	reduced continuum and core brightening.
2011.02.15	01:56	11158	S21 W14	X2.2	
2011.09.07	22:38	11283	N14 W30	X1.8	
2011.09.24	09:40	11302	N13 E61	X1.9	continuum brightening, core in emission.

2. Observations and Data Reduction

Since a strong correlation is known to exist between X-ray emission and observed continuum brightening (Neidig, 1989), we chose to analyze a large sample of candidate flares belonging to GOES X-ray class X6.9 to class C1.5. We primarily examined the HMI observables during the flares in order to establish the quantities most likely to be affected over the course of a flare, and their typical behavior. For this paper however, we only present observations from four representative X class flares that seem to best demonstrate the different observed photospheric effects: SOL2011-09-24T09:40, an X1.9 flare where the absorption line briefly goes into emission, with the line profile exhibiting a line width that changes with time; SOL2011-02-15T01:56, a X2.2 flare which shows noticeable reduction in line-depth, changes in the line width and less significant continuum brightening but for which the line does not go into emission; SOL2011-09-07T23:23, a X1.8 flare which shows distinct continuum brightening and even more pronounced line-core brightening, and, SOL2010-11-04T23:58:00, a M1.6 flare which shows line-core brightening but less significant continuum enhancement (See Table 1). We note that SOL2011-08-09T08:05:00, the strongest X class flare in the current solar cycle, also showed the line briefly going into emission.

The HMI instrument produces five line-of-sight (LOS) observables: pseudo-continuum intensity (I_c), Fe I line depth (L_d), line width (L_w), Doppler velocity (Dopplergrams, V), and LOS magnetic-field strength (magnetograms, M) every 45 seconds. In order to generate these quantities, HMI produces a nearly continuous stream of full-disc images of the Sun in a set of six narrow wavelength bands (FWHM 76 mÅ) clustered around the central wavelength of the Fe I photospheric absorption line at 6173Å (Schou *et al.*, 2012). Twelve filtergrams taken at six wavelengths and two polarizations (left-circular and right-circular, hereafter LCP and RCP) at a cadence of 3.75 seconds are used to calculate the HMI observables. However, it is important to note that the accuracy of these LOS observables is dependent on the algorithm used to translate a sequence of HMI filtergrams into corresponding observables. The algorithm used to calculate the continuum, line width and line depth assumes that the Fe I line is a "pure" Gaussian, and these quantities are obtained from analytical expressions using estimates of the first and second Fourier coefficients of the Fe I line profile

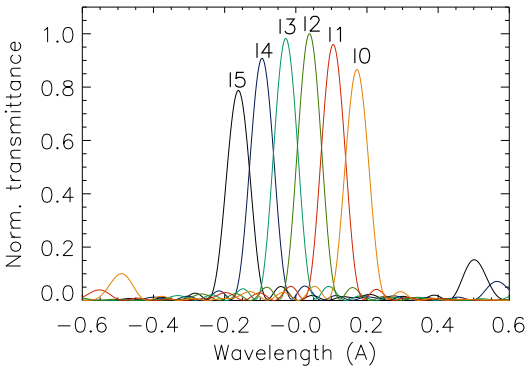

Figure 1. Spectral transmission profile of HMI Fe I line at 6173.34Å . Filtergrams are available at six wavelength positions (0.68mÅ apart) and two polarization states across the absorption line.

(Couvidat *et al.*, 2012). As such, these proxy quantities are more or less close to the actual observables, depending on the shape of the Fe I line at a specific HMI pixel and at a given time. However, in the presence of a strong magnetic field such as the one in a sunspot, or an active region, or during a flare, the LCP and RCP line profiles may be significantly different from a Gaussian profile. In such cases, the line width, line depth, and continuum intensities returned by the observables code might not bear much resemblance to the actual quantities and hence it is best to use only the filtergrams for quantitative measurements and analysis.

Since flares are impulsive phenomena often accompanied by changes in the local magnetic field; and it is known that algorithms used for calculating the observables under such conditions often yield spurious results, we use 45s cadence filtergrams taken at six equally-spaced (68.8 mÅ apart) tuning positions across the Fe I 6173.34 Å absorption line profile that have been tracked to the Carrington rate (see Figures 1 and 2). We do not use the raw level 1 filtergrams (which are separated by 3.75 seconds) but compute intermediate HMI data that have been interpolated in time to the same target time. Thus, the data used are based on the level 1 filtergrams separated by 3.75 seconds, but linearly interpolated to a specific time so that the twelve measurements all refer to the same target time. A gap-filling routine was also run, to spatially interpolate over bad pixels or cosmic ray hits. The tuning positions are at ± 34.4 mÅ (positions I3 and I2), ±103.2 mÅ (positions I4 and I1), and ±172.0 mÅ (positions I5 and I0) about the central wavelength of 6173.3433 Å (see Figure 1). As can be seen from Figures 1 and 2, the two wavelengths at ± 172.0 mÅ are close to the continuum when the Fe I line is at rest (i.e. Doppler velocity is zero.). However, when the velocity is different from zero, the line is shifted and in this case, only one of either I5 or I0 is a better estimate of the true continuum. Based on the Doppler velocity of the flaring region before the flare, we use the filtergram values of I5 (or I0) as the proxy continuum values.

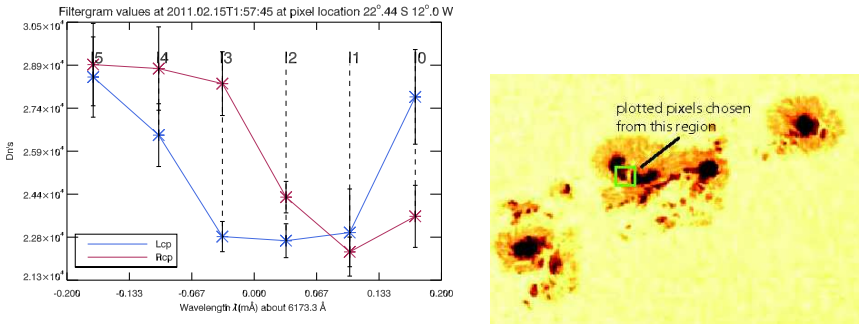

Figure 2. Top Left: The Left Circularly Polarized (LCP) and Right Circularly Polarized (RCP) spectral intensity values during SOL2011.02.15T1:56 at 2011.02.15_01:57:45 UTC for the pixel at 12°.00 W 22°.44 S. The presence of the magnetic field causes the shifts in the LCP and RCP line profiles (Zeeman Splitting) and the direction of the shift suggests that an average of I1 (i.e the average of LCP1 and RCP1) values would provide the best estimate of the line core. Doppler shift is positive, so I5 is our "proxy" continuum value. The error bars are $\pm 6\sigma$ and are calculated over the half hour interval before and after the flare. **Top Right:** The section of the active region AR 11158 selected for analysis.

Plots of the line profile during a flare (made using the LCP and RCP filtergrams values) exhibit the Zeeman splitting (see Figure 2) and can be used to determine the direction of the magnetic field. We use the plot to determine whether the intensity at I2, I3, an average of values at I1 and I2 or some combination thereof is a reasonable estimate for the "line core" value. We use the difference between this newly measured line core proxy and the continuum proxy as an estimate of the "line depth".

Image stabilization provides spatial stability of $0.03''$ throughout the complete sequences of filtergrams required for the observables. Typical per-pixel statistical noise for one filtergram is approximately 0.3%, as determined from time-series fluctuations away from the flare time. Exposure-time knowledge is about 0.002% and does not contribute to the error appreciably. For the continuum intensity measurement, combining all filtergrams over a 45 s frame sequence, the per-pixel noise is about 0.1%.

3. Discussion and Results

The plots in Figures 2-3 correspond to SOL2011-02-15T01:56:00 (X2.2). Figure 2 (left) shows the spectral intensity across the HMI line (Fe I 6173.34Å) during the flare in each of the polarization states (LCP and RCP). The Doppler velocity during the flare was positive and hence I5 (average of RCP5 and LCP5) values were taken as the proxy continuum values. The values at I1 (so average of RCP1 and LCP1) is deemed to best represent the line core. The error bars plotted are $\pm 6\sigma$ and have been calculated over a thirty minute interval before and after the flare. The image on the right shows the section of the active region AR 11158 chosen for analysis.

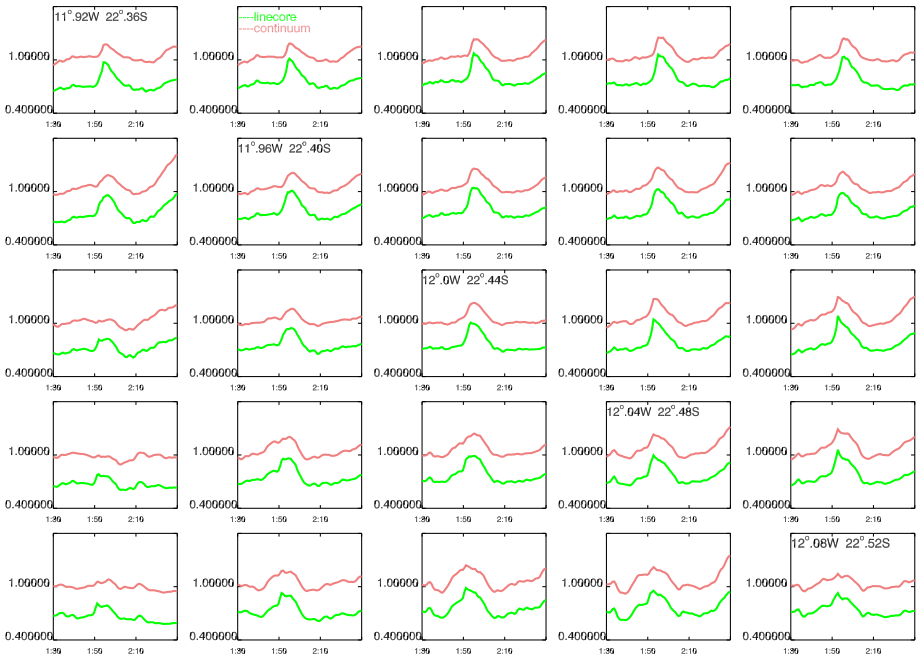

Figure 3. Mosaic of the time-variation plots of the normalized continuum (red) and line-core(green) intensity for a 5x5 pixel section of the active region of flare SOL2011-02-15T01:56:00. Each plot corresponds to a single pixel and the central pixel is located at 12°.00W 22°.44S. The horizontal axis spans a 60 min interval including the duration of the flare. The continuum and line-core values have been normalized by a linear fit of the continuum intensity 15 minutes before and after the flare. Note, the linear fit was performed to de-trend the effects of the spacecraft motion from the continuum and line-core data. Figure 2 shows the selected section of the active region.

Figure 3 shows a mosaic of temporal variations in the normalized continuum (red line) and line-core (green line) values for a grid of twenty-five pixels centered at 12°.0W, 22°.44S corresponding to the section shown in Figure 2 . Each plot corresponds to one pixel and the horizontal axis spans a period of sixty minutes (-including the flare) starting at 2011.02.15_01:30:00 UTC. The continuum and line core both have been normalized by a linear fit made using continuum data before and after the flare. Both continuum and line core were normalized by the same fit. This was done to both normalize the plots, and de-trend the effects of the spacecraft motion from the filtergram data. The central pixels show a distinct continuum and line core enhancements during the flare.

The images and plots in Figures 4-6 were created using filtergram data corresponding to SOL2011-09-07T22:38:00 (X1.8). Similar to Figure 3, Figure 4 illustrates the normalized temporal variation in the continuum and line core over a period of one hour (-including during the flare) in a 5x5 grid of twenty-five pixels centered at 13°.76N and 31°.84W. A large number of the pixels show greater than a 3-σ increase in the line core, but a more modest corresponding enhancement in the continuum value. Examination of all the pixels where the line core brightening was observed indicates that the line strength never ex-

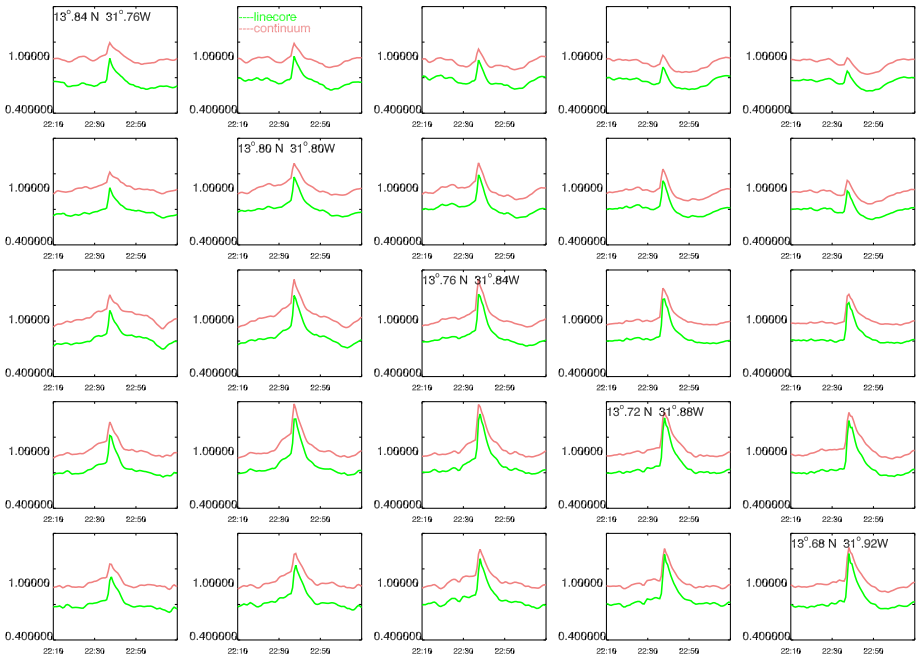

Figure 4. Mosaic of the time variation plots of the normalized continuum (red) and line-core(green) for a 5 x 5 pixel section of the active region that produced the flare SOL2011-09-07T22:38:00. Each plot corresponds to a single pixel. The central pixel is located at 13°.76N and 31°.84W. The horizontal (time) axis spans 60 min. The continuum and line-core values have been normalized to a linear fit of the continuum intensity 15 minutes before and after the flare. Note, the linear fit was performed to de-trend the spacecraft motion from the continuum and line-core data. Figure 6 shows the selected section of the active region.

ceeds the continuum and the line always stays in absorption for this flare. The Doppler velocity is positive and hence average I5 values are taken to represent the continuum values and the average of I2 and I1 (i.e. average of the values at RCP1, LCP1, RCP2, and LCP2) best represent the line-core values. Figure 5 is a typical time sequence of tracked and mapped images of the flaring "line core" as determined by averaging the filtergram values measured at I2 during the flare, and subtracting the preflare I2 image from that. These images are taken 45 s apart starting at 2011.09.07_22:36:15 UTC and are tracked to the Carrington rate. The last image is a continuum intensity image for the same region, provided for spatial reference. Figure 6 (left) shows the spectral intensity across the HMI line before and during the flare in both polarizations. I5 is the continuum approximation and I2 values best represents the line core. We note that a flattening of the line profile, consistent with the line-core increase exceeding the continuum increase, during the flare, with varying amplitude.

Figures 7-9 correspond to flare SOL2011-09-24T22:38:00 with Figure 7 showing the normalized continuum and line core plots centered at 12°.04 N and 61°.32 E. The Doppler velocity for this flare is negative; hence average of the values at position I0 are taken to best represent the continuum and average of the values at I2 and I3 best represents the line-core estimate. The mosaic of plots

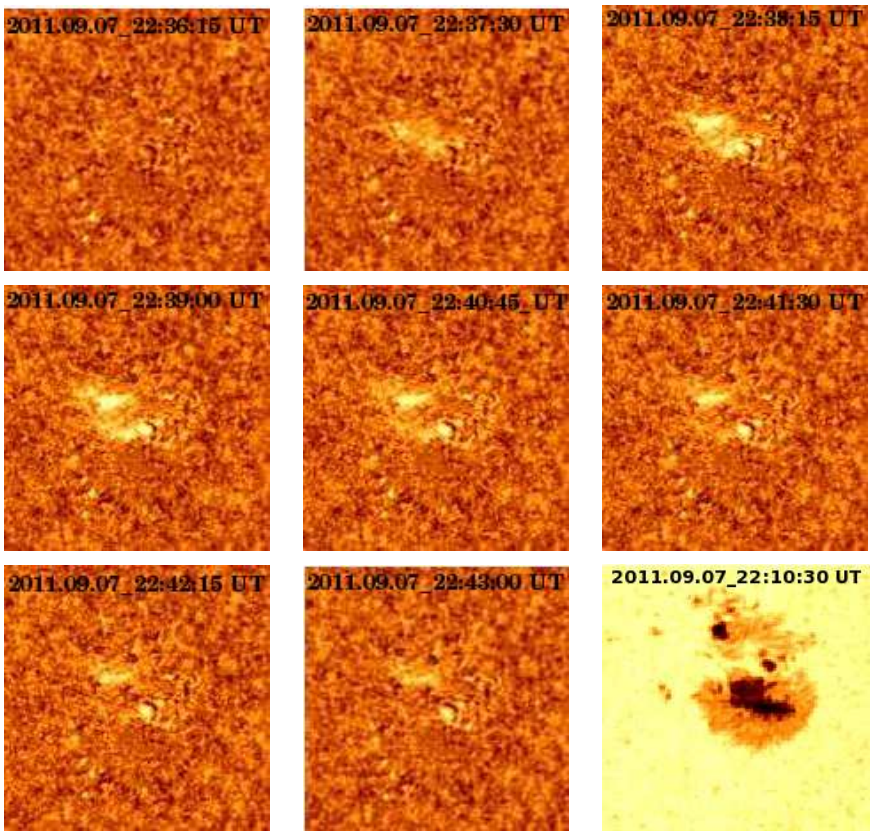

Figure 5. Brightening observed in the line-core images for SOL2011-09-07T22:38:00. These images have been produced by averaging the LCP and RCP filtergrams for wavelength positions corresponding to I2 and I1,i.e. corresponding to 6173.37Å and 6173.443Å which we assume to be a reasonable estimate of the "true" line-core intensity. The region shown is a 8.25° x 8.25° square, suitably tracked and mapped to a grid centered at 14°.0N and 30°.0W, the nominal location of the flare. The images shown are taken 45s apart starting at 2011.09.07_22:36:15 UT. The last image is a intensity image of the same region, provided for spatial reference.

show that the line-core equals of exceeds the continuum at many pixels and we see this phenomenon to last for more than ninety seconds. The horizontal axis in these plots is 90 minutes. Figure 9 shows the six spectral intensities (filtergrams) before and during the flare at two consecutive pixels located at 12°.08N and 61°.36E (left) and 12°.04 N 61°.32 E (right), demonstrating that the line width of the absorption line changes as a function of time over the duration of the flare. Temporal plots of the filtergrams show that, at some pixels, the absorption line core brightens as the flare progresses, and it temporarily exceeds the continuum: thus the absorption line reverses and actually goes into emission. Figure 8 is an image of the section of AR 11302 chosen for analysis. Past observations of flares (Babin and Koval, 2007; Lozitsky, 2009) suggest that while central emission features have been observed in the line-core before, such high

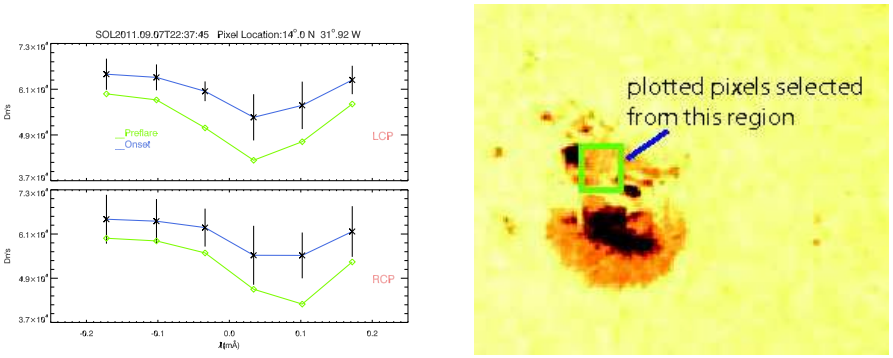

Figure 6. Top Left: Spectral intensity across the HMI line before (22:10:30:00 UTC, green color) and during the flare (22:37:45 UTC, blue color) for the pixel located at 13°.84N and 31°.72W. This pixel corresponds to the fourth pixel in the first column in the mosaic in Figures 4. Intensities in both left-circularly-polarized (LCP) and right-circularly-polarized (RCP) light are shown. The line-core values for this flare seem to be best represented by an average of values at I2 and I1. The Doppler velocity is positive, so I5 values best represent the continuum. The error bars represent ± six times the pre-flare standard deviation in the intensity values. **Top Right:** The section of the active region AR 11283 selected for analysis.

resolution observations of the entire line going into emission may be rare. We have observed similar line emission profiles in the flare SOL2011-08-09T08:05:00 (X6.9) suggesting they may be more common than believed in the past. The HMI white light flare SOL2010-06-12, as reported by Martínez Oliveros *et al.*, (2011) did not show this behavior.

Figures 8 and 9 show the corresponding plots and images for SOL2010-11-04T23:58:00 (M1.6). This is the the only M class flare ahown here but as the plots indicate, here too the line-core enhancement is more pronounced than the continuum enhancement.

Analysis of all X class flares observed by HMI (over nine so far), reveal that an increase in the continuum is observed in all the flares, suggesting that all the X-class flares could be categorized at white-light flares. However, the combination of an overall increase in brightness, and the reduced absorption in the line suggests that the line-core intensity responds more sensitively to the flare than the continuum intensity.

4. Summary

We have detected a photospheric continuum brightening in a large number of X ray flares. Many of these would traditionally have been classified as WLFs. However, the relative enhancement in the line-core profile is often significantly stronger than that observed in the continuum and is sometimes detectable even when there is no significant continuum enhancement. In a few cases, the line shape of the line changes so much during a flare that it line ceases to resemble a Gaussian. The line-core intensity sometimes temporarily exceeds the continuum

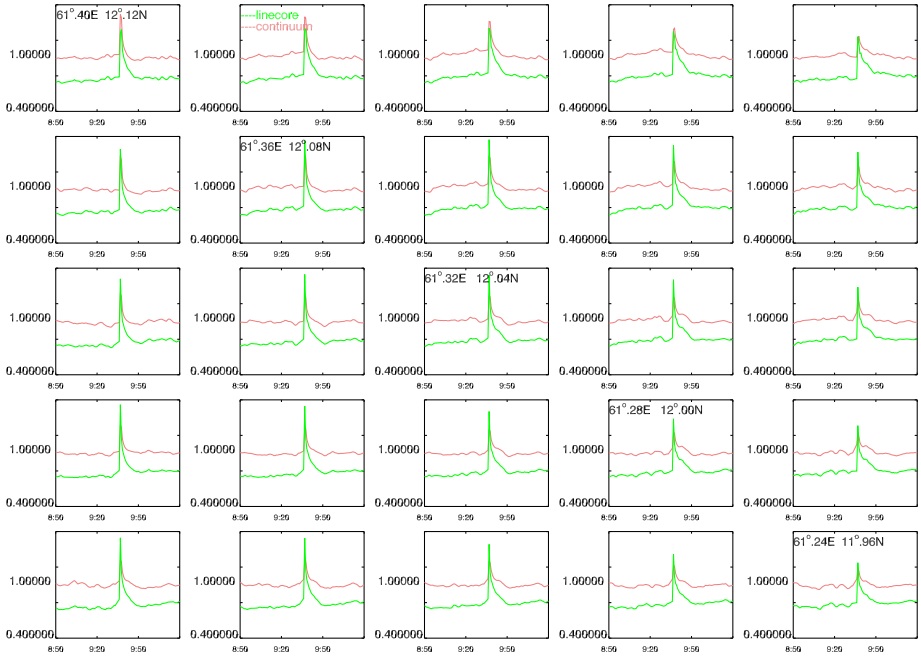

Figure 7. Mosaic of the time variation plots the normalized continuum (red)and line–core (green) intensity for a 5 x 5 section of the active region that produced the flare SOL2011-09-24T09:40:00. Each plot corresponds to a single pixel and the central pixel,is located at 61°.32 E and 12°.04 N. The horizontal (time) axis spans 120 min. The continuum and line-core values have been normalized to a linear fit of the continuum intensity 15 minutes before and after the flare. Note, the linear fit was performed to de-trend the effects of the spacecraft motion from the continuum and line-core data. Figure 8 shows the selected section of the active region .

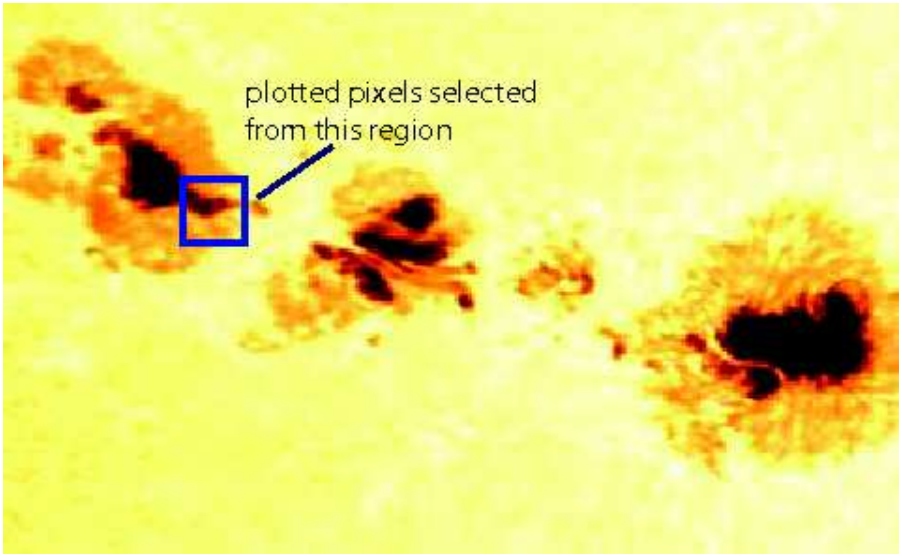

Figure 8. Section of active region AR 11302 selected for analysis.

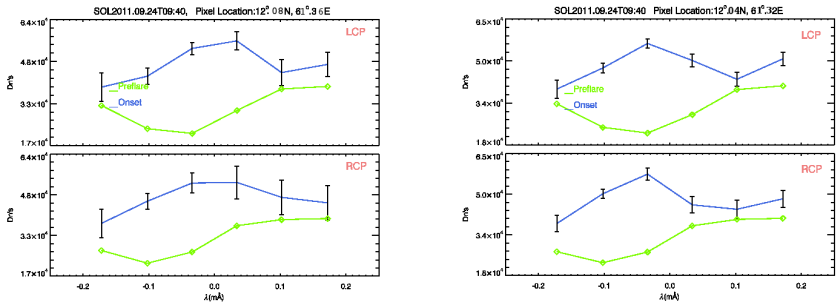

Figure 9. The six point spectral intensities (in LCP and RCP) of the pixels located at latitude $12^o.08$ N, $61^o.32$ E**(Top Left)** and $12^o.04$ N, $61^o.32$ E **(Top Right)** before and during the flare SOL2011-09-24T22:38:00. These "profiles" show that the line-core changes to a greater extent than the continuum during the flare, and the line goes briefly into emission. The Doppler velocity is negative and I0 is considered to be the best estimate of the true continuum with the average of I2 and I3 values as the best estimate of the linecore.

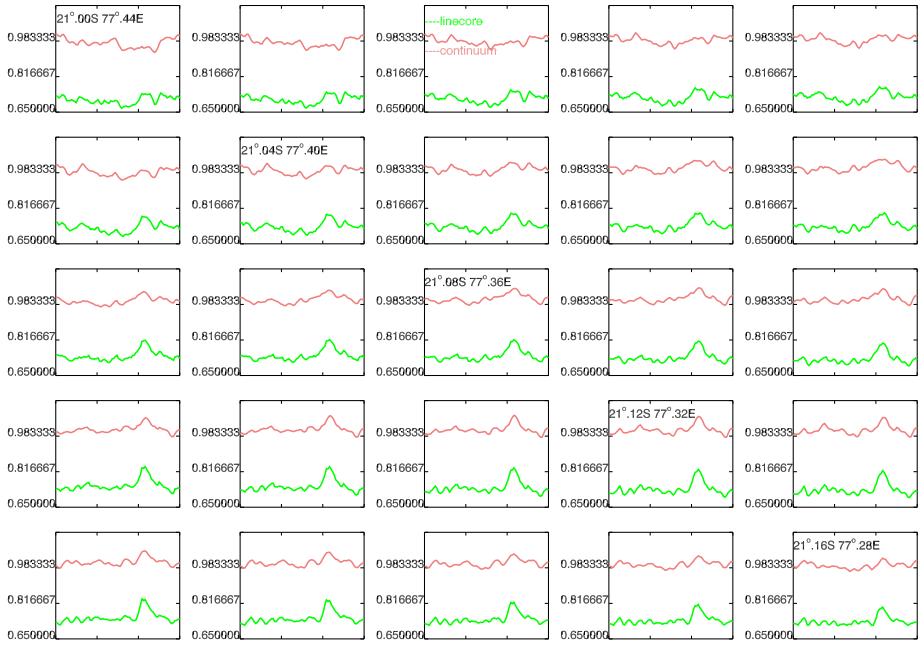

Figure 10. Mosaic of the time variation plots of normalized continuum and line core intensity for a 5 x 5 section of the active region that produced the flare SOL2010-11-04T23:58:00. Each plot corresponds to a single pixel,and the central pixel is located at $21^o.08$ S and $77^o.36$ E. The continuum and line-core values have been normalized to a linear fit of the continuum intensity 15 minutes before and after the flare. Note that the linear fit was performed to de-trend the effects of the spacecraft motion from the continuum and line-core data. The horizontal (time) axis spans 60 minutes. The selected region is shown in Figure 11.

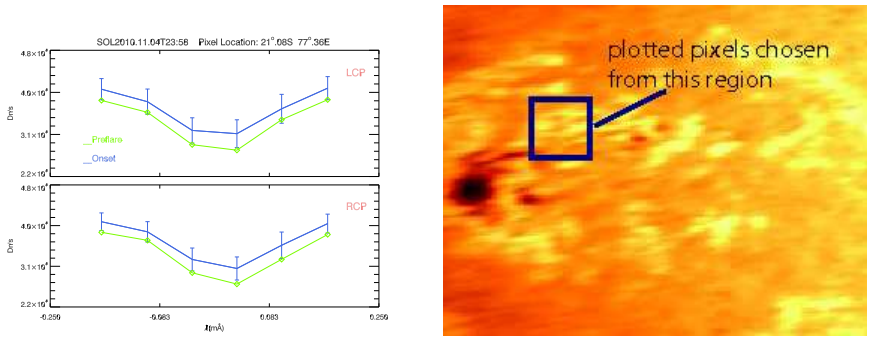

Figure 11. Top Left: The six point spectral intensities (in LCP and RCP) of the pixels located at latitude $21^o.08$ S and $77^o.36$ E before and during the flare SOL2011-09-24T22:38:00. This location corresponds to the central pixel in the mosaic in Figure 10. Doppler velocity is negative so I5 values are taken to represent the continuum. Average of values at I2 and I3 are assumed to best represent the line core. **Top Right:** The section of the active region AR 11121 corresponding to the pixels in Figure 10.

emission, thus reversing the absorption line into an emission line. The observed emission may last for over a minute before the line returns to absorption.

The flares so observed are spatially and temporally well correlated to the GOES X-ray events, indicating that HMI can be used to systematically study and track the photospheric effects of flares.

To study transient phenomenon like flares using HMI data, it is important to use level 1 HMI filtergrams instead of level 1.5 observables, since the algorithm used may yield spurious results in the presence of strong magnetic fields.

The flares studied show no tendency for circularly polarized radiation as a part of the continuum excess. We note this in passing because of occasional suggestions that synchrotron emission or other exotic mechanisms may play a role in the WLF continuum.

5. Acknowledgements

This work was supported by NASA Contract NAS5-02139 to Stanford University.

References

Babin, A.N., Koval, A.N.: 2007, Ni I 6768 Å line profile variations during a solar flare and their effect on the SOHO/MDI magnetic field measurements. *Bulletin Crimean Astrophysical Observatory* **103**, 63 – 68. doi:10.3103/S0190271707010093.

Carrington, R.C.: 1859, Description of a Singular Appearance seen in the Sun on September 1, 1859. *Mon. Not. Roy. Astron. Soc.* **20**, 13 – 15.

Couvidat, S., Rajaguru, S.P., Wachter, R., Sankarasubramanian, K., Schou, J., Scherrer, P.H.: 2012, Line-of-Sight Observables Algorithms for the Helioseismic and Magnetic Imager (HMI) Instrument Tested with Interferometric Bidimensional Spectrometer (IBIS) Observations. *Solar Phys.*, 13. doi:10.1007/s11207-011-9927-y.

Hudson, H.S., Wolfson, C.J., Metcalf, T.R.: 2006, White-Light Flares: A TRACE/RHESSI Overview. *Solar Phys.* **234**, 79 – 93. doi:10.1007/s11207-006-0056-y.

Jess, D.B., Mathioudakis, M., Crockett, P.J., Keenan, F.P.: 2008, Do All Flares Have White-Light Emission? *Astrophys. J. Lett.* **688**, L119 – L122. doi:10.1086/595588.

Lozitsky, V.G.: 2009, Magnetic fields and Fe I line profiles in the major solar flare on October 28, 2003. *Astronomy Letters* **35**, 136 – 142. doi:10.1134/S106377370902008X.

Martínez Oliveros, J.C., Couvidat, S., Schou, J., Krucker, S., Lindsey, C., Hudson, H.S., Scherrer, P.: 2011, Imaging Spectroscopy of a White-Light Solar Flare. *Solar Phys.* **269**, 269 – 281. doi:10.1007/s11207-010-9696-z.

Matthews, S.A., van Driel-Gesztelyi, L., Hudson, H.S., Nitta, N.V.: 2003, A catalogue of white-light flares observed by Yohkoh. *Astron. Astrophys.* **409**, 1107 – 1125. doi:10.1051/0004-6361:20031187.

Neidig, D.F.: 1989, The importance of solar white-light flares. *Solar Phys.* **121**, 261 – 269. doi:10.1007/BF00161699.

Neidig, D.F., Wiborg, P.H., Gilliam, L.B.: 1993, Physical properties of white-light flares derived from their center-to-limb distribution. *Solar Phys.* **144**, 169 – 194. doi:10.1007/BF00667990.

Schou, J., Scherrer, P.H., Bush, R.I., Wachter, R., Couvidat, S., Rabello-Soares, M.C., Bogart, R.S., Hoeksema, J.T., Liu, Y., Duvall, T.L., Akin, D.J., Allard, B.A., Miles, J.W., Rairden, R., Shine, R.A., Tarbell, T.D., Title, A.M., Wolfson, C.J., Elmore, D.F., Norton, A.A., Tomczyk, S.: 2012, Design and Ground Calibration of the Helioseismic and Magnetic Imager (HMI) Instrument on the Solar Dynamics Observatory (SDO). *Solar Phys.* **275**, 229 – 259. doi:10.1007/s11207-011-9842-2.

Wang, H.-M.: 2009, Study of white-light flares observed by Hinode. *Research in Astronomy and Astrophysics* **9**, 127 – 132. doi:10.1088/1674-4527/9/2/001.